# In Situ Measurements of Long-Lived Trace Gases in the Lower Stratosphere by Gas Chromatography

P. A. ROMASHKIN,*,+ D. F. HURST,*,+ J. W. ELKINS,* G. S. DUTTON,*,+ D. W. FAHEY,# R. E. DUNN,*,+,@ F. L. MOORE,*,+ R. C. MYERS,*,& AND B. D. HALL*

*NOAA/Climate Monitoring and Diagnostics Laboratory, Boulder, Colorado
+CIRES, University of Colorado, Boulder, Colorado
#NOAA/Aeronomy Laboratory, Boulder, Colorado

(Manuscript received 28 August 2000, in final form 7 December 2000)

ABSTRACT

Detailed information on the four-channel Airborne Chromatograph for Atmospheric Trace Species (ACATS-IV), used to measure long-lived atmospheric trace gases, is presented. Since ACATS-IV was last described in the literature, the temporal resolution of some measurements was tripled during 1997–99, chromatography was significantly changed, and data processing improved. ACATS-IV presently measures $CCl_3F$ [chlorofluorocarbon (CFC)-11], $CCl_2FCClF_2$ (CFC-113), $CH_3CCl_3$ (methyl chloroform), $CCl_4$ (carbon tetrachloride), $CH_4$ (methane), $H_2$ (hydrogen), and $CHCl_3$ (chloroform) every 140 s, and $N_2O$ (nitrous oxide), $CCl_2F_2$ (CFC-12), $CBrClF_2$ (halon-1211), and $SF_6$ (sulfur hexafluoride) every 70 s. An in-depth description of the instrument operation, standardization, calibration, and data processing is provided, along with a discussion of precision and uncertainties of ambient air measurements for several airborne missions.

## 1. Introduction

Environmental regulations concerning potentially harmful compounds released into the atmosphere require understanding and prediction of the rate of stratospheric ozone loss, greenhouse gas increase and large-scale atmospheric circulation. The Montreal and Kyoto Protocols have emphasized the importance of stratospheric measurements of ozone-depleting and greenhouse gases. Expansion of ground-based monitoring networks (Elkins et al. 1996a; Fraser et al. 1996; Hartley et al. 1996; Montzka 1996, and others) along with improvements in measurement technology provide increasingly accurate records of tropospheric mixing ratios and emissions evaluations. Tropical advection and subsequent poleward stratospheric transport and mixing (Brewer 1949; Dobson 1956; Murgatroyd and Singleton 1961) redistribute long-lived trace gases released at the surface. Accurate measurements of these gases in the stratosphere, combined with the documented tropospheric history, provide valuable information on stratospheric loss of trace gases, release of ozone-depleting radicals, stratospheric transport, mixing, and troposphere–stratosphere exchange (Rood et al. 1992; Volk et al. 1996). These characteristics are essential for understanding atmospheric dynamics and chemistry and predicting ozone loss.

Airborne Chromatograph for Atmospheric Trace Species (ACATS) instruments data back to 1991, when the first single-channel in situ airborne gas chromatograph was developed (see Woodbridge et al. 1995). ACATS-IV, a four-channel in situ gas chromatograph (Elkins et al. 1996b), was first deployed during the 1994 Airborne Southern Hemisphere Ozone Experiment/Measurements for Assessing the Effects of Stratospheric Aviation (ASHOE/MAESA) campaign. It also has been a part of the National Aeronautics and Space Administration (NASA) ER-2 aircraft payload during 1996 Stratospheric Tracers of Atmospheric Transport (STRAT), 1997 Photochemistry of Ozone Loss in Arctic Regions in Summer (POLARIS) and 2000 Stratospheric Aerosol and Gas Experiment (SAGE-III) Ozone Loss and Validation Experiment (SOLVE) missions. Since last described by Elkins et al. (1996b), the ACATS-IV sampling rate has been increased to 70–140 s, following the replacement of two chromatography columns and the addition of a postcolumn (see section 2 below). To enable faster chromatography, carrier gas flow programming was implemented. A separate air intake pump has been added, replacing the pump shared with the reactive

@ Current affiliation: Dynojet Research, Inc., Belgrade, Montana.
& Current affiliation: Analytical Chemistry Division, NIST, Gaithersburg, Maryland.

*Corresponding author address:* Dr. Pavel A. Romashkin, Climate Monitoring and Diagnostics Laboratory, NOAA, 325 Broadway, Boulder, CO 80303-3328.
E-mail: promashkin@cmdl.noaa.gov

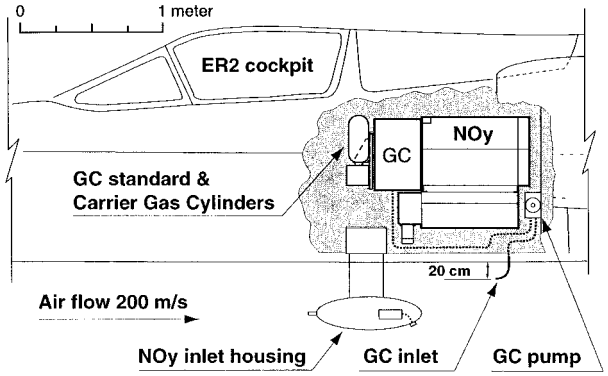


FIG. 1. Location of the ACATS-IV instrument next to the reactive nitrogen instrument (NOy) inside the lower instrument bay (Q-bay) of the ER-2 aircraft. The components of the gas chromatograph (GC) system are the ACATS-IV GC itself, inlet, pump and standard and carrier gas cylinders.

nitrogen (NOy) instrument (Fahey et al. 1995). The ability to take measurements in the troposphere was added by providing vacuum to the exhaust of the detectors and sample loops, and controlling the intake pump from the ACATS-IV computer.

Trace gas measurements at relatively high temporal resolution are the main products of ACATS-IV. These measurements provide information on the number of important atmospheric features, such as mean age of air parcels, total chlorine and bromine loading of the stratosphere, and partitioning of halogen pools.

## 2. Instrument

ACATS-IV is a four-channel gas chromatograph that measures $CCl_3F$ [chlorofluorocarbon (CFC)-11], $CCl_2FCClF_2$ (CFC-113), $CH_3CCl_3$ (methyl chloroform), $CCl_4$ (carbon tetrachloride), $CH_4$ (methane), $H_2$ (hydrogen), and $CHCl_3$ (chloroform) every 140 s. $N_2O$ (nitrous oxide), $CCl_2F_2$ (CFC-12), $CBrClF_2$ (halon-1211), and $SF_6$ (sulfur hexafluoride) are measured every 70 s. ACATS-IV operates as follows.

Air external to the aircraft is delivered to the instrument by an external, variable speed, two-stage, Teflon diaphragm pump (KNF Neuberger), driven by a brushless 28-V DC motor. The pump is mounted on the aft wall of the ER-2 Q-bay (Fig. 1) and is turned on by the ACATS-IV onboard computer when the ER-2 aircraft ascends through 87 kPa of atmospheric pressure. Ambient air is routed through about 2 m of the 4.5-mm internal diameter (ID) stainless steel tubing from outside the aircraft fuselage to the series of sample loops inside the instrument (Fig. 1, dashed lines). The flow of the air through the sample loops is limited to about 180 sccm (standard cubic centimeters per minute) by using an absolute pressure relief valve (Tavco, set to about 150 kPa). Sample flow is measured and recorded through the flight to ensure adequate flushing of sample loops.

All samples throughout a flight are injected at the same sample loop pressure. To achieve this, the loops prior to the injection of a sample are isolated from the pump [using solenoid valve (SV) 6, Fig. 2] and allowed to depressurize through the exhaust, lightweight, proprietary pressure controller (PC) 1, (Fig. 2) to 87 kPa. All pressure controllers of ACATS-IV are identical (PC1–PC5. Fig. 2), rely upon a pressure gradient across them, and will not function properly unless the exhaust pressure is sufficiently lower than the inlet pressure. Therefore, to make measurements in the troposphere, where the ambient pressure is close to 87 kPa, a miniature diaphragm pump (KNF Neuberger, 24-V brushless DC motor, model UNMP30) is used to provide the consistent exhaust vacuum to all five pressure controllers.

About 9 s after SV6 is closed, the desired pressure is reached in the sample loops and they are isolated from the exhaust using SV5 (Fig. 2). Sample injection pressure (measured by the pressure controller) and temperature are recorded for later normalization of detector responses. Then, samples are injected onto each chromatography column using a 12-port, two-position gas sampling valve (GSV; Valco model EWC12TGA).

Two packed chromatography columns are employed per channel: a precolumn and main column, selected to rapidly separate compounds of interest. Channel 1 also employs a short, 0.15-m postcolumn, operating at higher temperature than pre- and main columns (Table 1, Fig. 2) to separate $N_2O$ and $SF_6$. Detectors and columns for each chromatography channel are enclosed in individual, thin-walled, insulated aluminum housings (ovens) and are heated using 50–100-W electric heaters. Temperature control of the ovens is crucial for the stability of chromatography, and is accomplished by using nine computer-interfaced controllers (Omega Engineering, Inc., Stamford, Connecticut, model CN76122-485), one for each of the detectors and chromatography columns. Temperature variations are within $\pm 0.1^{\circ}$C. The characteristics of columns are shown in Table 1 and channel configurations are shown in Table 2.

The instrument detects part per trillion (ppt) levels of gases of interest in the ambient air samples using electron-capture detectors (ECDs). Channels 1–3 use Valco ECDs (model 140BN by Valco Instruments Co. Inc., Houston, Texas) and channel 4 uses a Shimadzu ECD (Shimadzu GC-mini-2, Tokyo, Japan). Carrier gases are ultrahigh purity (UHP; 99.999%) $N_2$ for channels 2–4 and UHP P-5 (argon + 5% methane) for channel 1. Channel 4 is doped with about 30 parts per million (ppm) dry mole fraction $N_2O$ to enhance the detection of $H_2$ and methane. The ECD signals are sampled at 8 Hz. Exhaust pressures of the ECDs are controlled by pressure controllers PC2–PC5 (Fig. 2), to prevent flows through ECDs from changing in response to ambient pressure fluctuations during the flight.

Fast rate of measurements is achieved in ACATS-IV through the use of a chromatographic technique, defined

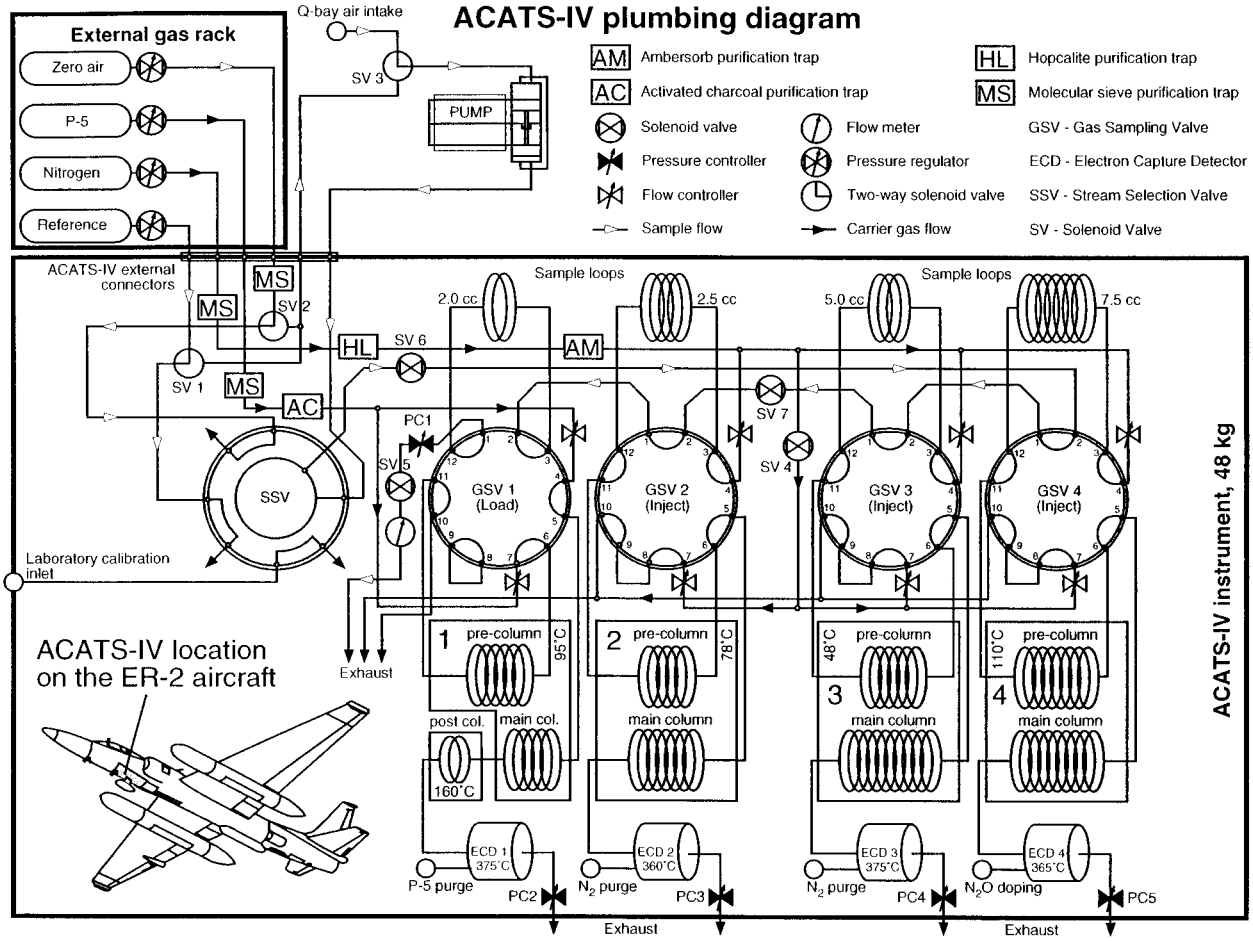


FIG. 2. Plumbing diagram of the ACATS-IV instrument. ACATS-IV is connected to the external pump, delivering outside air to the instrument, and rack carrying compressed gas bottles. Solenoid values (SVs) are as follows: Reference gas through the pump divert (SV1), zero-air through the pump divert (SV2), pump stream selection (SV3), nitrogen backflush cutoff (SV4), sample loop out cutoff (SV5), sample loop in cutoff (SV6), and P-5 backstream cutoff (SV7). Gas sampling valves (GSVs) 2–4 are shown in ''inject'' position, allowing sample air from the loops to enter the chromatography columns. GSV1 is in ''load'' position, allowing the sample loop to fill with sample air.

here as ''foldback'' chromatography, which allows the next sample to be injected soon after late-eluting gases from the previous sample injection leave the precolumn and enter the main chromatographic column (Fig. 3). With foldback, late-eluting peaks from a previous injection lie on a nearly flat baseline in front of the air peak of the next injection. Foldback is implemented on the ACATS-IV channels 3 and 4 ($CH_3CCl_3$, $CCl_4$ and $CH_4$, Table 2, Fig. 4), reducing the time between injections to 140 s, while the length of chromatograms remains at 210 s. Channels 1 and 2 ($N_2O$, $SF_6$ halon-1211, and CFC-12) have chromatogram lengths of 70 s and do not use foldback.

Foldback requires precise timing of GSV switches so that late-eluting molecules can pass completely through the precolumn before it is backflushed by switching a GSV into the ''load'' position (Fig. 2, GSV 1). Backflushing, the passing of carrier gas through precolumns in the direction opposite to the normal flow, is necessary to expel from the precolumn all molecules eluting later than peaks of interest. The next sample can then be injected onto a clean precolumn. The fact that precolumns are in use until the last eluting peaks are transferred into main columns leaves a very short time (30 s) to backflush them. Sufficient backflushing is achieved if the volume of flushing carrier gas is at least 1.5 times the volume of carrier gas passed through a precolumn in the ''forward'' direction. Therefore, backflush flow rates are maintained as high as 90–100 sccm. Although providing adequate precolumn cleansing, the high backflush flows create strong inverted pressure gradients in the precolumns that hinder the forward carrier gas flow through the precolumn/main column series when the GSV is switched into the ''inject'' position. The resulting drop in the forward flow through columns and ECDs produces an increase of the baseline of the chromatogram, which can be detrimental to the detection of overlaying foldback chromatographic peaks. To accelerate the recovery of forward flow rates, the forward carrier gas flow at injection time is increased up to 200

TABLE 1. Characteristics of chromatographic columns of the ACATS-IV instrument. All columns are stainless steel.

| Channel no. | Internal diameter (mm) | Precolumn material | Length (m) | Main column material | Length (m) | Temperature (°C) | Molecules measured |
|---|---|---|---|---|---|---|---|
| 1* | 1.8 | Porapak Q | 0.6 | Porapak Q | 1.8 | 95 | $SF_6$, $N_2O$ |
| 2 | 2.2 | 20% OV-101 on Chromosorb | 1.2 | 20% OV-101 on Chromosorb | 3.6 | 78 | CFC-12, halon-1211 |
| 3 | 2.2 | 3% OV-101 on Chromosorb | 1.2 | 3% OV-101 on Chromosorb | 3.6 | 48 | CFC-11, CFC-113, $CHCl_3$, $CH_3CCl_3$, $CCl_4$ |
| 4 | 3.8 | Unibeads 1S | 2.0 | Molecular Sieve 5A | 3.3 | 110 | $H_2$, $CH_4$ |

* Configuration of channel 1 includes 0.15-m-long postcolumn packed with Molecular Sieve 5A, operated at 160°C, plumbed directly after main column.

sccm for 4–7 s, and then decreased back to normal in a series of steps. This carrier gas flow programming helps remove baseline aberrations that can affect the foldback peaks. Flow programming is performed using proprietary low-weight mass flow controllers controlled by the instrument computer.

Even with sophisticated flow programming, the high sensitivity of ECDs to small carrier gas flow changes sometimes results in disturbances of the baseline under foldback peaks (Fig. 4, Channel 3, dashed lines). These small changes in the baseline can make consistent integration of the peaks difficult for some molecules ($CH_3CCl_3$, $CCl_4$) and may increase the uncertainty of the measurements. To remedy this problem, baseline subtraction is performed prior to peak integration for these molecules. The ''clean'' baseline (with no analyte peaks) is obtained from zero-air (from Scott–Marrin Company, California) injections, which are performed under conditions identical to ambient air injections (Fig. 4, dashed lines). Baseline subtraction proved necessary only for channel 3, where the detection of $CH_3CCl_3$ and $CCl_4$ is complicated by a baseline increase (Fig. 4, channel 3). See section 4 below for details of the integration and zero-air subtraction methods.

The serial arrangement of sample loops (Fig. 2) made it possible for P-5 carrier gas (pressurized at 620 kPa, compared to 87 kPa sample pressure) from precolumn 1 to backstream into sample loop 4 (which is used to measure methane), once GSV 1 switches into the ''load'' position. The 5% $CH_4$ concentration in P-5 causes methane contamination of the sample on channel 4. To prevent this, a solenoid valve (SV7, Fig. 2) is used to isolate sample loops 1 and 2 from loops 3 and 4. The valve, SV7, is programmed to close shortly before the switching of GSV to ''load'' on channel 1, and remains closed for 12 s until the P-5 carrier gas bleeds out of sample loops. After that, SV7 is opened and all loops are filled and flushed with sample air.

ACATS-IV measures 84 cm × 49 cm × 33 cm, weighs 48 kg and is installed on the ER-2 aircraft next to the NOy instrument inside a common frame. The frame also supports a compressed gas cylinder rack with pressurized, 3- and 1.5-L, Aculife-IV (Scott Specialty Gases, Plumsteadville, Pennsylvania) treated, Kevlar-reinforced, aluminum bottles that contain ACATS-IV and NOy carrier gases (Fig. 1). An additional 1.5-L external gas bottle was added to the underside of the ACATS-IV instrument in 2000 due to increased demand on the nitrogen carrier gas caused by faster chromatography. The entire ACATS-IV–NOy assembly is mounted to three support eyelets in the instrument bay (Q-bay) in the bottom forward section of the ER-2 aircraft fuselage (Figs. 1 and 2, inset).

The instrument operation is preprogrammed to allow automatic in-flight analyses of ambient air from outside the aircraft, a standard gas, and zero-air from the gas rack. Instrument control and data acquisition are handled by an onboard Intel 486-based computer. More details on the injection sequence are provided in section 4.

## 3. Calibration

The response of ECDs to halocarbons is sometimes nonlinear, especially for larger peaks that approach the saturation limit of the detectors, or asymmetrical peaks (Table 2). The only molecules measured by ACATS-IV that exhibit noticeable nonlinearity are CFC-11, $CH_4$, and $H_2$. To accurately measure mixing ratios from high tropospheric to near-zero stratospheric values during the course of a flight, any nonlinearity needs to be taken into account. Therefore, ACATS-IV is calibrated on the ground using zero-air and secondary standards that span the expected range of mixing ratios (Elkins et al. 1996b; Elkins et al. 1993). Secondary standards were made by diluting dried tropospheric air collected in 1994 and 1996 at Niwot Ridge, Colorado, by 20%–80% with ultrapure (not containing measurable amounts of gases of interest) zero-air. All secondary standards are calibrated against primary gravimetric standards (Montzka et al. 1993; Novelli et al. 1991) prepared and maintained by the Climate Monitoring and Diagnostics Laboratory in Boulder, Colorado (see Table 3). The calibration of the ACATS-IV instrument was performed at least once during each field deployment, or more frequently if changes to the chromatography or the instrument were made. Calibrations involve measuring at least four standards, including the standard used during the flight, and a zero-air, which is scrubbed of most of the measured mole-

TABLE 2. ACATS-IV channel configuration in 1997. Instrument responses shown are approximate. The instrumental precision during POLARIS is $\sigma_{inst}$ (see section 5). Precision of measurements is the median reported precision for a given mission, relative to the measured mixing ratios.

| Channel [injection cycle(s)] | Compound name | Molecular formula | Retention time (s) | Response[a] (Hz) ± $\sigma_{inst}$ | Overall reported uncertainty[d] (%) | | | |
|---|---|---|---|---|---|---|---|---|
| | | | | | ASHOE/MAESA | STRAT | POLARIS | SOLVE |
| 1 | Sulfur hexafluoride | $SF_6$ | 35 | 200 ± 1.14% | 1.34 | 1.68 | 4.56 | 2.75 |
| (70) | Nitrous oxide | $N_2O$ | 46 | 12 800 ± 0.50% | 0.94 | 1.47 | 0.72 | 0.32 |
| 2 | CFC-12 | $CCl_2F_2$ | 52 | 31 600 ± 0.13% | 0.82 | 2.06 | 1.01 | 0.49 |
| (70) | Halon-1211 | $CBrClF_2$ | 63.5 | 1500 ± 1.53% | 2.65 | 4.72 | 5.88 | 1.43 |
| 3 | CFC-11 | $CCl_3F$ | 77.5 | 51 000 ± 0.09% | 0.33 | 1.72 | 1.02 | 0.38 |
| (140) | CFC-113 | $CCl_2FCClF_2$ | 87 | 5200 ± 0.31% | 1.63 | 1.77 | 1.74 | 0.47 |
| | Chloroform | $CHCl_3$ | 118 | 110 ± 4.78% | N/A | N/A | 22.08 | 21.33 |
| | Methyl chloroform[b] | $CH_3CCl_3$ | 144 | 2200 ± 0.33% | 1.02 | 2.10 | 2.04 | 0.91 |
| | Carbon tetrachloride[b] | $CCl_4$ | 163 | 8100 ± 0.45% | 1.31 | 2.08 | 1.52 | 0.55 |
| 4 | Hydrogen | $H_2$ | 67 | 300 ± 2.48% | 3.58[c] | 2.21[c] | 2.71[c] | 7.64 |
| (140) | Methane[b] | $CH_4$ | 163 | 3000 ± 1.10% | 1.77 | 1.98 | 2.32 | 0.49 |

[a] The response shown is to the injection of tropospheric ambient air with mixing ratios similar to those in KLM-1574 in Table 3.
[b] Molecule eluts after the injection of the next sample (foldback; see explanation in section 2).
[c] Uncertainty of measurements using peak area. All other uncertainties are using peak height. After 1998, peak height is used to measure $H_2$.
[d] Accuracy is estimated at < 2% plus precision (Elkins et al. 1996b).




FIG. 3. Injection timing used in (A) normal and (B) foldback chromatography. State of the associated gas sampling valve (GSV) is shown below each panel. High state is ''inject'' position, low state is ''load,'' or backflush, position. In (A) there is a flat area in front of the shaded air peak, while in (B) injections occur more frequently so that late eluting peaks overlap this flat section.

cules. Instrument responses to the four standards are normalized to the response of the in-flight standard gas (KLM-1566 during POLARIS and SOLVE). The four standard and zero-air measurements are plotted against their mixing ratios and fit with a quadratic function (cubic for CFC-11, Fig. 5) to produce a calibration curve, such as that shown in Fig. 6. For most measured compounds, the residuals of fitting range from $<0.5\%$ ($N_2O$) to 2% (CFC-11). For $SF_6$ and $H_2$, the residuals reach 4% and for $CHCl_3$ they reach up to 15%, due to small peak size.

The compounds $SF_6$ and $N_2O$ could not be completely removed from the zero-air used to calibrate the instrument, voiding zero-air calibration points for these molecules. Calibration curves for these gases are based on four standard measurements, with the lowest one at 0.5 ppt of $SF_6$ and 60.4 parts per billion (ppb) dry mole fraction of $N_2O$. This could cause larger errors for $SF_6$ and $N_2O$ below these limits (about 20% of the 1994 surface tropospheric average, Table 3). However, stratospheric mixing ratios of $N_2O$ and $SF_6$ observed at the ER-2 cruise altitudes are well above these values, and the precision of measurements is not compromised.

The ECD response to CFC-11 is highly nonlinear, and a quadratic calibration curve does not adequately

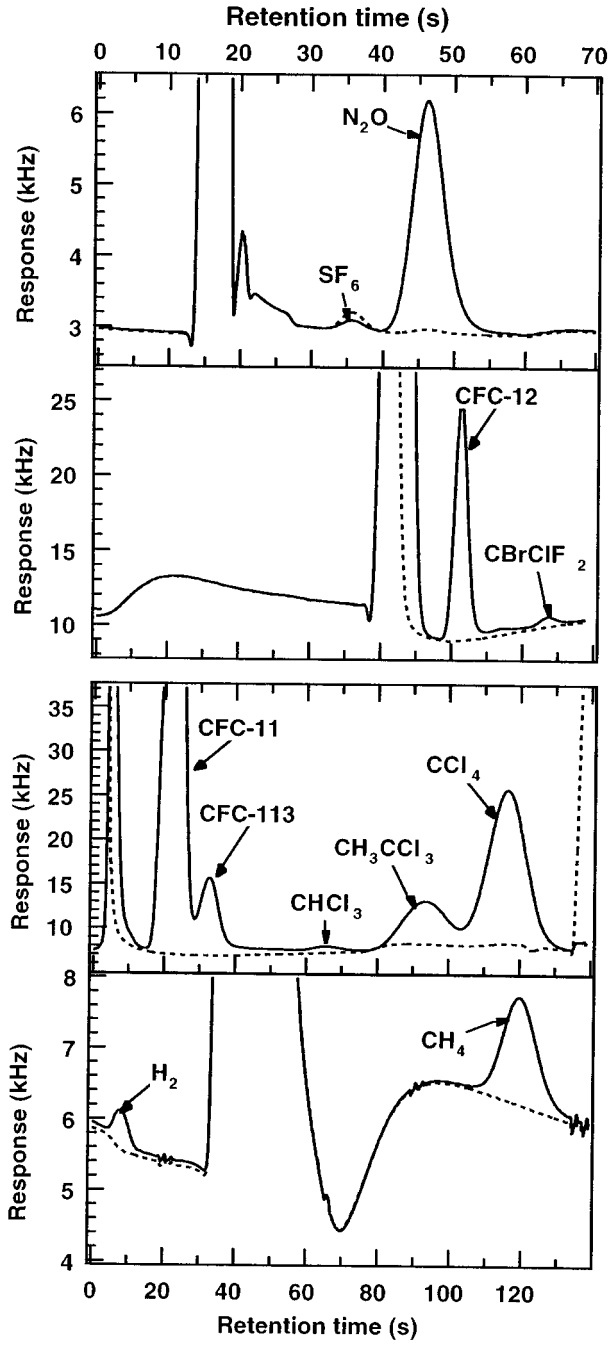


FIG. 4. Example chromatograms from 11 Mar 2000 flight. Zero-air (dashed line) provides a reference baseline. On channel 3, it is subtracted from sampled air chromatogram (solid line) to simplify peak edge detection of methyl chloroform and carbon tetrachloride. Folded-back methyl chloroform, carbon tetrachloride, and methane peaks were moved from the beginning of the next chromatogram to the end of current chromatogram. High $SF_6$ content in zero-air does not affect measurements because baseline subtraction is not employed on this channel.

represent tropospheric mixing ratios (Fig. 5). Using quadratic calibration curves for calculating CFC-11 mixing ratios in the upper troposphere during STRAT and POLARIS in 1996–97 produced unrealistically high CFC-11 values. The problem was recognized during POLARIS and corrected by creating cubic (third-order polynomial) calibration curves for CFC-11 (Fig. 5). Using cubic calibration curves proved unnecessary for compounds measured by ACATS-IV that exhibit only a slight nonlinearity, such as $CH_4$ and $H_2$ (see Fig. 6 for examples of calibration curves), so standard quadratic curves are used.

Calibration data are handled with IGOR Pro (WaveMetrics Inc., Lake Oswego, Oregon) and, recently, Interactive Data Language (IDL; Research Systems Inc., Boulder, Colorado) software on a Macintosh G4 personal computer. Proprietary code has been developed for calibration data reduction and making the calibration curves. Separate calibration curves are made for both measured heights and areas of the chromatographic peaks (see section 4). The curves providing the least scatter of measurements for repeated injections of the same sample gas (typically those using peak height) are used in the actual flight data processing.

## 4. Data collection and processing

During a flight, ACATS-IV operation is controlled and monitored by an onboard computer and an array of sensors. Gas flows and pressures, temperatures of ECDs, sample loops, and internal components are measured and recorded at rates up to 1 Hz. These engineering data, along with the chromatograms, are stored on a 40-Mb PCMCIA FlashDisk (solid-state removable memory card).

For data processing, in-flight standard gas and zero-air measurements are used to correct for drifts in detector responses caused by pressure and temperature changes, and to check and correct for possible sample contamination. Figure 7, showing typical ACATS-IV flight data, illustrates the injection sequence. During a flight, ACATS-IV injects one standard gas sample for every seven ambient air samples, and a zero-air sample for every 40 injections. Standard gas injections monitor the changes in the detector response throughout the flight, so that the responses to the ambient air are constrained by standard gas measurements.

As mentioned in section 2, the baseline of the folded back chromatograms may have small variations due to fluctuations of carrier gas flows through the ECDs. Zero-air injections on channel 3 produce clean chromatogram baselines with no analyte peaks, which can be used for baseline subtraction to improve peak detection of $CH_3CCl_3$ and $CCl_4$. Zero-air injections can also help detect and allow correction of internal sample contamination. Also, at least two samples of zero-air and standard gas per flight are passed through the sampling pump (''pump divert,'' shown as diamonds on Fig. 2)

TABLE 3. Reference gas values used for calibrating ACATS-IV during ASHOE/MAESA, STRAT, and POLARIS. Reference gases were produced by diluting ambient tropospheric air from Niwot Ridge, Colorado, with zero-air (approximate percentage of ambient tropospheric value in parenthesis). Boldface indicates standards used during 1997 POLARIS campaign and lightface indicates previously used gases that are currently used only for quality control.

| Compound | Units* | KLM-1223 (57%) | KLM-1441 (48%) | KLM-1492 (97%) | KLM-1493 (34%) | **KLM-1496 (20%)** | **KLM-1500 (34%)** | **KLM-1566 (83%)** | **KLM-1574 (100%)** |
|---|---|---|---|---|---|---|---|---|---|
| CFC-11 | ppt | 156.9 | 131.0 | 266.9 | 94.3 | **54.2** | **93.9** | **226.7** | **273.4** |
| CFC-12 | ppt | 297.0 | 248.2 | 506.1 | 180.8 | **102.5** | **180.7** | **437.8** | **535.7** |
| CFC-113 | ppt | 48.6 | 40.9 | 80.7 | 28.9 | **17.3** | **29.1** | **76.0** | **82.5** |
| $CH_3CCl_3$ | ppt | 79.8 | 67.9 | 126.1 | 46.6 | **24.9** | **45.1** | **86.2** | **107.6** |
| $CCl_4$ | ppt | 59.9 | 49.4 | 101.2 | 35.9 | **20.1** | **35.6** | **85.3** | **102.6** |
| $CHCl_3$ | ppt | 7.9 | 6.6 | — | 3.4 | **2.2** | **4.6** | **14.7** | **20.0** |
| $CBrClF_2$ | ppt | 1.85 | 1.57 | 3.40 | 1.17 | **0.62** | **1.15** | **3.18** | **3.81** |
| $N_2O$ | ppb | 177 | 148.3 | 301.7 | 106.8 | **60.4** | **106.5** | **258.7** | **314.6** |
| $SF_6$ | ppt | 1.92 | 1.60 | 3.2 | 1.06 | **0.58** | **1.06** | **3.28** | **4.02** |
| $CH_4$ | ppb | 1058.8 | 876.8 | 1705.4 | 599.7 | **338.9** | **596.9** | **1508.2** | **1857.0** |
| $H_2$ | ppb | 297 | 247 | 533 | 157 | **112** | **158** | **429** | **522** |

* Measurement units are parts per trillion (ppt) or parts per billion (ppb) dry mole fraction.

and analyzed. Pump diverts of zero-air reveal any contamination occurring in the pump or sampling lines. Such pump contamination of $CH_3CCl_3$ and $CCl_4$ occurred a few times during POLARIS and was traced to the aluminum intake pump heads and corrected. By injecting a standard gas through the pump, a possible loss of compounds of interest to the pump or external plumbing can be quantified and corrected. No noticeable loss to the components of the intake system was ever detected.

Data processing is handled by custom programs for IGOR Pro and in IDL. During data processing, the fold-back chromatograms are first ''unfolded,'' that is, the 55-s-long beginning of each chromatogram on channels 3 and 4 is moved to the end of the previous chromatogram to obtain full-length chromatograms for each injection. Second, chromatograms are smoothed to remove high-frequency (>2 Hz) noise, using the Savitzky–Golay method. Third, the peak edges of each species in a chromatogram are detected, typically by matching the tangents on both edges of a peak with the slope between these edges. This rather laborious but fully automated method is necessary because of highly compact chromatograms that sometimes have sloping baselines, co-eluting peaks, widely varying mixing ratios, and small (<1–2 s) drift in retention times. After the peak edges are detected, they can be displayed for visual control. Next, peaks are integrated and both their area and height over the baseline are normalized to standard temperature and pressure, using the measured pressure and temperature of the sample loops (recorded during the flight). On channel 3, CFC-11, CFC-113, and chloroform peaks are integrated first, then the interpolated zero-air chromatograms are subtracted from ambient air chromatograms, and $CH_3CCl_3$ and $CCl_4$ are processed.

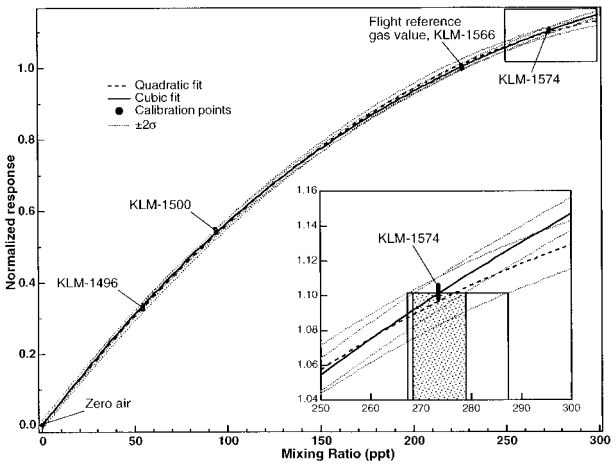


FIG. 5. CFC-11 calibration curves. The inset shows that a quadratic least squares fit (dashed line) does not describe measurements very well: it can be seen that it does not go through KLM-1574. Uncertainty of the quadratic fit (unfilled rectangle) in the 100%-ambient air region are nearly twice that of the cubic fit (solid line and shaded rectangle), which matches KLM-1574 measurements better. Current midlatitude Northern Hemisphere tropospheric value of CFC-11 is about 270 ppt.

After peak integration is completed, the time series of standard gas measurements (shown as squares on Fig. 7) is smoothed, typically using a three-point Gaussian method, and the root-mean-square (rms) of the residuals of smoothing is calculated. This rms represents the measurement precision for each compound during the flight. After smoothing, standard gas measurements are linearly interpolated to the frequency of ambient air measurements to produce the reference time series. Area and height responses of the integrated ambient air peaks are divided by the corresponding interpolated standard gas values, and the results are stored for subsequent mixing ratio calculations using the calibration curves.

For molecules measured by ACATS-IV, the precision is higher for peak heights than for peak areas, because peak height is inherently easier to measure and relies less on accurate peak edge detection that may suffer from baseline noise. However, peak area was used prior to 1999 to calculate the mixing ratio of hydrogen, which

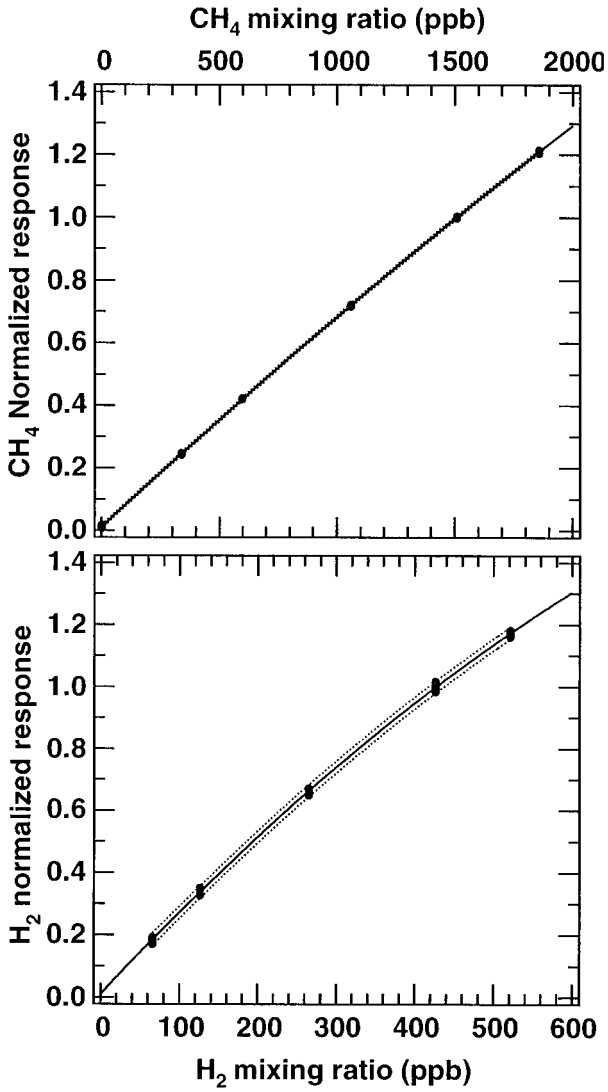


FIG. 6. $CH_4$ and $H_2$ calibration curves are the only two ACATS-IV molecules other than CFC-11 that display noticeable nonlinearity. Only slight nonlinearity is present, in $CH_4$ and $H_2$, so second-order polynomial fits are used to create calibration curves. Uncertainty is higher for $H_2$, which is a much smaller peak than $CH_4$.

produced a small and sometimes flat-topped peak, the crest of which cannot be identified unambiguously. In 1999 the $N_2O$ doping level was optimized on channel 4, resulting in a higher and more Gaussian $H_2$ peak, allowing the use of peak height for $H_2$ mixing ratio calculations.

Even at a 210-s chromatogram length, CFC-11 and CFC-113, $CH_3CCl_3$ and $CCl_4$ are not completely resolved. For $CH_3CCl_3$ and $CCl_4$, this does not significantly affect the precision of measurements because mixing ratios of both compounds vary similarly with altitude due to their comparable photolytic lifetimes (Volk et al. 1997). Calibration of the instrument, which is performed under the same conditions and for the similar range of mixing ratios as sample analyses, incorporates the effect of co-elution. For CFC-11 and CFC-113, the lifetimes of which differ in the stratosphere and the mixing ratios of which change radically, precautions are taken to avoid biasing caused by peak overlap. Mixing ratios of both compounds are evaluated based on peak height measured from a calculated straight line extending from the beginning of the CFC-11 peak to the end of the CFC-113 peak. This way, the degree of separation (''valley'' depth) between the peaks has little influence on the inferred mixing ratios. The same technique was tested for the $CH_3CCl_3$ and $CCl_4$ pair, but the increase in precision was insignificant. Ambient air mixing ratios are calculated from the normalized responses for each compound in each air sample, either by iteratively looking up mixing ratios using cubic (third order) calibration curves (CFC-11) or solving the quadratic (second order) calibration equations (all other species). This step allows visual evaluation of calibration curves, normalized ambient air responses, and final mixing ratios.

As mentioned above, ACATS-IV relies upon an external pump and over 2 m of a 4.5-mm ID stainless steel tubing to sample ambient air from outside the ER-2 fuselage and compress the sample to the required injection pressure of 87 kPa. Considering the low (5 kPa) ambient pressures at the 20 km ER-2 cruise altitude, pumping results in a delay between the intake of the sample and the actual time of injection. This delay is computed before creating final data files by analyzing the anticorrelation between CFC-11 and the in situ ozone measurements from the ER-2-based ozone photometer (Proffitt et al. 1989). This approach is based on the fact that, in the midlatitude stratosphere, with increasing altitude, CFC-11 is photolytically destroyed and its mixing ratio decreases, while the ozone mixing ratio increases, showing strong anticorrelation. For polar air masses with considerable ozone loss, the correlation between $N_2O$ and $CO_2$ measurements is used instead. To obtain the correction time, 120 correlations are computed over a $\pm$60-s window centered at the time stamp provided by the ACATS-IV clock. The time at which the lowest anticorrelation coefficient is found is considered the correction value. Such correlation with $O_3$ measurements also eliminates discrepancies between the instruments clocks, which occurred during POLARIS. Although the pump delay is typically about 15 s, each flight's time stamps are corrected individually by 10–60 s, as the result of internal clock offsets between the instruments that vary from flight to flight. Possible pump delay variations throughout the same flight are not significant given the sampling frequency of ACATS-IV of 70–140 s.

## 5. Precision and accuracy

The total uncertainty, $E_{\text{total}} = (\sigma^2_{\text{flight}} + \sigma^2_{\text{cal}})^{1/2} + E_{\text{cal}}$, of the ACATS-IV measurements has three components:

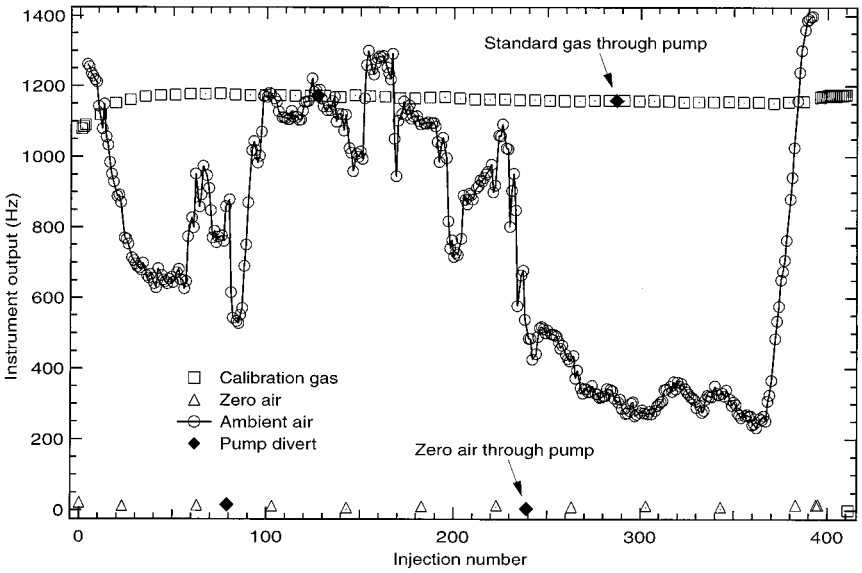


FIG. 7. Example of an ACATS-IV flight profile ($N_2O$ from 11 Mar 2000 flight). Standard gas measurements (rectangles) are smoothed and interpolated to the frequency of ambient air measurements (circles) for normalization during data processing. Fluctuations in the ambient air response are driven by the ER-2 aircraft diving into the troposphere and ascending into the stratosphere, and by crossing the boundaries between midlatitude and polar vortex air masses where strong variability of $N_2O$ was observed.

the uncertainty of in-flight standard gas measurements $\sigma_{\text{flight}}$ the precision of calibration curves $\sigma_{\text{cal}}$, and inaccuracy of standard gas values $E_{\text{cal}}$. Uncertainty of in-flight calibration stems from the fact that detector responses change slightly during the instrument warm-up, and vary throughout a flight due to slightly changing temperature, pressure etc. These response changes can cause a drift of the in-flight calibration, particularly at the beginning of the flight (solid squares on Fig. 7) as well as noise in calibrations throughout the flight. In-flight calibration precision $\sigma_{\text{flight}}$ of ACATS-IV measurements is defined as the rms of the residuals of smoothing of the in-flight standard gas responses (see section 4).

Calibration uncertainty $\sigma_{\text{cal}}$ is attributable mostly to the noise in the repeated measurements of at least four standard gases over the time required to complete a calibration experiment (notice vertical spread in data points on the cutout, Fig. 5). Inaccuracy of standard gas values $E_{\text{cal}}$ also contributes to $\sigma_{\text{cal}}$ because the goodness of fitting is limited by the accuracy of mixing ratios assigned to standard gases [$E_{\text{cal}}$ is estimated $<2\%$ plus precision (Elkins et al. 1996b)]. Unconstrained lower ends of the calibration curves (e.g., $SF_6$ and $N_2O$; see section 3) with high errors are insignificant sources of uncertainty in measurements, because atmospheric mixing ratios are always higher than the mixing ratio of the lowest standard used to produce the calibration curve. This is the case for all of the ACATS-IV molecules except $SF_6$. Present-day sulfur hexafluoride measurements are not constrained by the 1994 tropospheric value used for making calibration curves, due to the continued atmospheric growth of $SF_6$. However, ambient air measurements of $SF_6$ are not affected noticeably because of the linear response of the ECD to this molecule.

As described in section 3, third-order calibration curves for CFC-11 were used for STRAT and preliminary POLARIS datasets. To simplify error calculations, the calibration curve uncertainties contributing to the overall reported CFC-11 measurement error (Table 2) are based on the quadratic calibration curves and, as such, are slightly exaggerated for the CFC-11 mixing ratios above 265 ppt.

The overall reported ACATS-IV uncertainties ($E_{\text{total}}$ as in the equation above 1, not including $E_{\text{cal}}$) are calculated individually for every ambient air measurement throughout a flight in mixing ratio units (ppt or ppb), because the precision of the in-flight calibration measurements $\sigma_{\text{flight}}$, varies between flights, and the calibration curve uncertainty $\sigma_{\text{cal}}$ is mixing-ratio dependent. Summaries of ACATS-IV uncertainties for ASHOE/MAESA, STRAT, and POLARIS are provided in Table 2. Greater uncertainties during POLARIS are due to the experimentation with the foldback chromatography, which affected both the in-flight calibration measurements and calibration curve uncertainties.

The instrumental precision $\sigma_{\text{inst}}$ (values during POLARIS are shown in Table 2), defined as the ability of the instrument to reproduce the same detector response to repeated injections of the identical samples, is expressed as 1 $\sigma$ about the expected value. The instru-

mental precision is inseparable from the two uncertainties discussed above and contributes to them in the amount specified in Table 2. The instrumental precision includes the short-term (<10 min) deviations in temperature and carrier gas flows, electronic noise, and other similar factors determined by the characteristics of instrument components.

The accuracy of the ACATS-IV measurements is determined by the accuracy of the secondary standards used to calibrate the instrument, and is estimated at $<\pm 2\%$ plus precision (Elkins et al. 1996b).

*Acknowledgments.* We acknowledge the Lockheed–Martin engineering and field support staff, and the ER-2 aircraft pilots for operating airborne missions. ACATS-IV was funded in part by the NASA Upper Atmospheric Research Program (UARP), the Atmospheric Effects of Stratospheric Aircraft Project (AESA) of the NASA High Speed Research Program (HSRP), and the Atmospheric Chemistry Project of the NOAA Climate and Global Change (C&GC) Program.

## REFERENCES

Brewer, A. W., 1949: Evidence for a world circulation provided by measurements of helium and water vapor distribution in the stratosphere. *Quart. J. Roy. Meteor. Soc.,* **75,** 351–363.

Dobson, G. M. G., 1956: Origin and distribution of polyatomic molecules in the atmosphere. *Proc. Roy. Soc. London,* **236A,** 187–193.

Elkins, J. W., T. M. Thompson, T. H. Swanson, J. H. Butler, B. D. Hall, S. O. Cummings, D. A. Fisher, and A. G. Raffo, 1993: Decrease in the growth rates of atmospheric chlorofluorocarbons 11 and 12. *Nature,* **364,** 780–783.

——, and Coauthors, 1996a: Nitrous oxide and halocompounds. Climate Monitoring and Diagnostics Laboratory Summary Rep. 23, U.S. Dept. of Commerce, Boulder, CO, 84–111.

——, and Coauthors, 1996b: Airborne gas chromatograph for in situ measurements of long-lived species in the upper troposphere and lower stratosphere. *Geophys. Res. Lett.,* **23** (4), 347–350.

Fahey, D. W., and Coauthors, 1995: In situ observations in aircraft exhaust plumes in the lower stratosphere at midlatitudes. *J. Geophys. Res.,* **100** (D2), 3065–3072.

Fraser, P., D. Cunnold, F. Alyea, R. Weiss, R. Prinn, P. Simmonds, B. Miller, and R. Langenfelds, 1996: Lifetime and emission estimates of 1,1,2-trichlorotrifluorethane (CFC-113) from daily global background observations June 1982–June 1994. *J. Geophys. Res.,* **101** (D7), 12 585–12 599.

Hartley, D. E., T. Kindler, D. E. Cunnold, and R. G. Prinn, 1996: Evaluating chemical transport models: Comparison of effects of different CFC-11 emission scenarios. *J. Geophys. Res.,* **101,** 14 381–14 385.

Montzka, S. A., R. C. Myers, J. H. Butler, S. C. Cummings, and J. W. Elkins, 1993: Global tropospheric distribution and calibration scale of HCFC-22. *Geophys. Res. Lett.,* **20** (8), 703–706.

——, J. H. Butler, R. C. Myers, T. M. Thompson, T. H. Swanson, A. D. Clarke, L. T. Lock, and J. W. Elkins, 1996: Decline in the tropospheric abundance of halogen from halocarbons: Implications for stratospheric ozone depletion. *Science,* **272,** 1318–1322.

Murgatroyd, R. J., and F. Singleton, 1961: Possible meridional circulations in the stratosphere and mesosphere. *Quart. J. Roy. Meteor. Soc.,* **87,** 125–135.

Novelli, P. C., J. W. Elkins, and L. P. Steele, 1991: The development and evaluation of a gravimetric reference scale for measurements of atmospheric carbon monoxide. *J. Geophys. Res.,* **96** (D7), 13 109–13 121.

Proffitt, M. H., and Coauthors, 1989: In-situ measurements within the 1987 Antarctic ozone hole from a high-altitude ER-2 aircraft. *J. Geophys. Res.,* **94** (D14), 16 547–16 555.

Rood, R. B., J. E. Nielsen, R. S. Stolarski, A. R. Douglass, J. A. Kaye, and D. J. Allen, 1992: Episodic total ozone minima and associated effects on heterogeneous chemistry and lower stratospheric transport. *J. Geophys. Res.,* **97** (D8), 7979–7996.

Volk, C. M., and Coauthors, 1996: Quantifying transport between the tropical and mid-latitude lower stratosphere. *Science,* **272,** 1763–1768.

——, and Coauthors, 1997: Evaluation of source gas lifetimes from stratospheric observations. *J. Geophys. Res.,* **102** (D21), 25 543–25 564.

Woodbridge, E. L., and Coauthors, 1995: Estimates of total organic and inorganic chlorine in the lower stratosphere from *in situ* and flask measurements. *J. Geophys. Res.,* **100** (D2), 3057–3064.